Published in final edited form as:
Calcif Tissue Int. 2009 September ; 85(3): 235–246. doi:10.1007/s00223-009-9270-6.

Survey of the Enthesopathy of X-Linked Hypophosphatemia and Its Characterization in Hyp Mice

Guoying Liang,
Department of Internal Medicine/Endocrinology, Yale University, P.O. Box 208020, New Haven, CT 06520-8020, USA

Lee D. Katz,
Department of Diagnostic Radiology, Yale University, New Haven, CT, USA

Karl L. Insogna,
Department of Internal Medicine/Endocrinology, Yale University, P.O. Box 208020, New Haven, CT 06520-8020, USA

Thomas O. Carpenter, and
Department of Pediatrics, Yale University, New Haven, CT, USA

Carolyn M. Macica
Department of Internal Medicine/Endocrinology, Yale University, P.O. Box 208020, New Haven, CT 06520-8020, USA

Carolyn M. Macica: carolyn.macica@yale.edu

Abstract

X-linked hypophosphatemia (XLH) is characterized by rickets and osteomalacia as a result of an inactivating mutation of the PHEX (phosphate-regulating gene with homology to endopeptidases on the X chromosome) gene. PHEX encodes an endopeptidase that, when inactivated, results in elevated circulating levels of FGF-23, a novel phosphate-regulating hormone (a phosphatonin), thereby resulting in increased phosphate excretion and impaired bone mineralization. A generalized and severe mineralizing enthesopathy in patients with XLH was first reported in 1985; we likewise report a survey in which we found evidence of enthesopathy in fibrocartilaginous insertion sites, as well as osteophyte formation, in the majority of patients. Nonetheless, there has been very little focus on the progression and pathogenesis underlying the paradoxical heterotopic calcification of tendon and ligament insertion sites. Such studies have been hampered by lack of a model of mineralizing enthesopathy. We therefore characterized the involvement of the most frequently targeted fibrocartilaginous tendon insertion sites in Hyp mice, a murine model of the XLH mutation that phenocopies the human syndrome in every detail including hypophosphatemia and elevated FGF-23. Histological examination of the affected entheses revealed that mineralizing insertion sites, while thought to involve bone spur formation, were not due to bone-forming osteoblasts but instead to a significant expansion of mineralizing fibrocartilage. Our finding that enthesis fibrocartilage cells specifically express fibroblast growth factor receptor 3 (FGFR3)/Klotho suggests that the high circulating levels of FGF-23, characteristic of XLH and Hyp mice, may be part of the biochemical milieu that underlies the expansion of mineralizing enthesis fibrocartilage.

Keywords

Rickets; Osteomalacia; Ectopic calcification; Ligaments; Tendons

Correspondence to: Carolyn M. Macica, carolyn.macica@yale.edu.

The characteristic hypophosphatemia of X-linked hypophosphatemia (XLH) arises as a consequence of a defective PHEX (phosphate-regulating gene with homology to endopeptidases on the X chromosome) gene product, which ultimately results in impaired proximal tubule phosphate reabsorption. In addition, despite severe hypophosphatemia, 1,25-dihydroxyvitamin D_3 ($1,25[OH]_2D_3$) production is not appropriately enhanced, due to FGF-23-mediated suppression of 1α-hydroxylase activity. A number of phosphate-wasting disorders phenotypically similar to XLH have been attributed to high circulating levels of FGF-23, including tumor-induced osteomalacia (TIO), autosomal dominant hypophosphatemic rickets (ADHR), and autosomal recessive hypophosphatemic rickets (ARHR) [1–5].

Despite the characteristic osteomalacia of XLH, there is a paradoxical heterotopic calcification of tendon and ligament insertion sites, a manifestation of the disease described over 20 years ago [6,7]. These manifestations are of considerable clinical importance in that they may limit functional range of motion and are often painful. Tendon and ligament insertions are categorized as either fibrous or fibrocartilaginous, the latter characterized by both unmineralized and mineralized zones of fibrocartilage cells and most often the subject of injury [8]. In the general aging population or in “overuse” injuries, the two most common reported bony changes are osteophytes and enthesophytes [9]. *Osteophytes* are lateral outgrowths of bone at the margin of the articular surface of a synovial joint; *enthesophytes* are bony spur formations at a ligament or tendon insertion into bone. We confirmed a generalized enthesopathy/osteophytopathy in a clinical survey of over 30 patients affected with XLH; calcaneal spurs and Achilles enthesopathy are often affected earlier than other sites. These aforementioned changes associated with XLH do not appear to be determined by phosphate/calcitriol treatment and are therefore likely intrinsic to the basic disease process [10]. However, there are no studies to date that examine either the progression or pathogenesis underlying the mineralization of insertion sites in humans with XLH. These studies have been hampered by the lack of a model of mineralizing enthesopathy/osteophytopathy. We have therefore characterized several fibrocartilaginous entheses for phenotypic changes consistent with mineralization of insertion sites observed in XLH, using a murine model of the disorder (Hyp mice). Involved sites include the Achilles tendon insertion of the triceps surae into the calcaneus, the quadriceps femoris tendon insertion into the patella, and the patellar attachment of the patellar ligament that attaches to the tibial tubercle. We also examined the profile of candidate FGF-23 receptors in fibrocartilaginous entheses to address the potential role that elevated FGF-23 levels might play in the pathogenesis of enthesopathy.

Materials and Methods

Chemicals

All chemical reagents were obtained from Sigma-Aldrich (St. Louis, MO) unless otherwise indicated. FGFR1, FGFR3, and type II collagen antibodies were obtained from Abcam (Cambridge, MA); and Klotho antibody was from Lifespan Biosciences (Seattle, WA).

Animals and Tissue Processing

Female Hyp mice of the C57BL/6 strain (and age-matched C57BL/6 controls) were obtained in-house in the Yale University School of Medicine Animal Care Facility using animals obtained from Jackson Laboratories (Bar Harbor, ME) or retired breeders (and age-matched controls) obtained from Jackson Laboratories. All animals were maintained on normal rat chow and in accordance with the NIH’s *Guide for the Care and Use of Laboratory Animals*. Osteomalacia was confirmed in each sample by examining the tibia of control and Hyp mice, which showed characteristic expanded type II collagen-positive cartilage in the residual growth plate and in subarticular and trabecular bone regions (data not shown). Because of the

progressive nature of enthesophyte formation in XLH, we studied the entheses of older adult mice (6–8 months of age), unless otherwise indicated. Sites processed were the Achilles tendon insertion of the triceps surae (gastrocnemius and soleus muscles) into the calcaneus, the quadriceps femoris tendon insertion (rectus femoris, vastus lateralis, vastus medialis, and vastus intermedius muscles) into the patella, and the patellar tendon that inserts into the tibial tubercle. Bones were rapidly dissected, being careful to preserve the muscle/tendon/enthesis insertion structure. Tissues were fixed in 4% PBS-buffered paraformaldehyde (PFA) for 1–2 hours on ice. Selected bones were decalcified in daily changes of 7% EDTA/PBS solution at pH 7.1 for 14 days at 4°C and washed with PBS/50 mM $MgCl_2$ overnight. Tissues were paraffin-embedded and sectioned to a thickness of 8 μm, with the section thickness used as an indicator of relative tissue depth for comparison between Hyp and control fibrocartilaginous insertion sites. Each condition was repeated in eight age-matched mice (four for type X collagen staining). Serial sections were used for each designated insertion for Masson's trichrome staining and to measure alkaline phosphatase (AP) and type II collagen staining. The contralateral leg was embedded in plastic and used for von Kossa staining.

For immunohistochemistry, tissue sections were deparaffinized with Histoclear® (National Diagnostics, Atlanta, GA) and rehydrated, and epitope retrieval was performed by enzymatic retrieval (pepsin [Lab Vision, Fremont, CA] for type II collagen antibody, trypsin [Chemicon, Temecula, CA] for FGFR and type X antibodies, protease I [Ventana Medical Systems, Tucson, AZ] for Klotho antibody) for 10 min at 37°C. Sections were quenched for endogenous peroxidase activity (0.3% H_2O_2 in methanol) for 10 min and blocked for 1 hour with serum. Sections were incubated for 1 hour at room temperature with the indicated antibody. Sections were washed, and immunostaining was visualized using the ABC staining system (Vector Labs, Burlingame, CA), followed by incubation with peroxidase substrate (DAB chromagen) for 3–5 min.

AP Activity and von Kossa Staining

AP was measured in deparaffinized sections, rehydrated, and incubated for 1 hour in Tris buffer (pH 9.4). Slides were stained for 1 hour at 37°C in a solution of 0.02 g/mL fast blue, 0.02 g/mL naphthol ASBI phosphate, and 0.05% $MgCl_2$ in 39 mL (pH 9.4) Tris buffer. Sections were rinsed and mounted with aqueous mountant. AP activity between control mice and the expanded fibrocartilage of Hyp mice was compared and expressed as a percentage of AP-positive cells in the enthesis to the total area of either the calcaneus or patella (mean ± SD). Bone mineral staining was conducted in 1 μm plastic-embedded sections by the Yale Core Center for Musculoskeletal Disorders (YCCMD) employing a von Kossa staining procedure with toluidine blue counterstaining.

Masson's Trichrome Staining

Sections were deparaffinized, rehydrated, and placed in Bouin's solution at room temperature overnight. Slides were washed and stained in working Weigert's iron hematoxylin solution for 5 min, then washed and stained in Biebrich scarlet-acid fuchsin for 5 min. Slides were then incubated in phosphomolybdic/phosphotungstic acid solution (1:1:2 dH_2O) for 5–10 min. Sections were subsequently stained in aniline blue solution (2.4% aniline blue, 2% acetic acid) for 5 min. Slides were briefly washed in distilled water and placed in 1% acetic acid solution for 3–5 min, followed by dehydration to Histoclear and mounted. Masson's stain colors collagen and bone blue (bone matrix stains more deeply) and muscle red. Masson's stain was also used as a readout of postnatal Achilles organ maturation into mature, matrix-secreting fibrocartilaginous insertion into the calcaneus.

FGF-23 Assay

Circulating levels of FGF-23 were measured using an ELISA method that detects the intact molecule (Kainos Laboratories, Tokyo, Japan).

Human Subjects

Radiographic studies of 39 subjects affected with XLH, 9–75 years of age, were performed as part of a natural history/phenotyping study ongoing at the Yale Center for X-Linked Hypophosphatemia. Films of the thoracic and lumbar spine were not taken in subjects 18 years of age or less. The study protocol was approved by the Yale Human Investigation and Radiation Safety Committees; all subjects provided informed consent prior to participation.

Results

A Mineralizing Enthesopathy Is Pervasive in XLH

In a survey of 39 patients with XLH (32.7 ± 19.5 years) the majority had evidence of enthesopathy. The predominant sites involved were the knees, ankles, pelvis, and thoracic spine. Involvement was usually bilateral for the shoulder, elbow, knee, ankle, and hand sites; and the number of sites involved increased with age. The frequency of involvement at the sites examined radiographically is shown in Table 1. Examples of the ossification of the Achilles and patellar tendons are shown in Fig. 1.

Enthesis Fibrocartilage Is Greatly Expanded in Hyp Mice

An understanding of the cellular events leading to the progression of inappropriate mineralization of enthesis in XLH would be greatly fostered by the availability of an animal model. We therefore conducted studies characterizing several fibrocartilaginous insertion sites commonly affected in XLH using Hyp mice, a murine model of XLH that manifests the characteristic physiological and biochemical features of the disorder, including hypophosphatemia, excess urinary renal phosphate excretion, rickets, and osteomalacia. Tendon/ligament insertion sites are characterized as being either fibrous or fibrocartilaginous depending on the bone–tendon interface [8]. Because the involvement of fibrous insertion sites in enthesopathies is relatively limited, we focused our attention on several prototypical fibrocartilaginous entheses in mice, including the Achilles tendon and patellar insertions. These sites are especially prone to pathological changes in metabolic disorders such as XLH, as well as in repetitive strain injuries and age-related changes [9,11,12]. Enthesis fibrocartilage cells are phenotypically identified as rounded cells arranged in rows that are separated by collagen fibers [13]. Using Masson's trichrome metachromatic stain (collagen/bone stains blue), we found that, in contrast to control age-matched mice, the fibrocartilage of Hyp mice was greatly expanded along the posterior calcaneal tuberosity (Fig. 2a and c, respectively). In addition, compared to control mice, fibrocartilage of Hyp mice was observed deep into the medial process of the tuberosity, into the plantar fascia ligament attachment (Fig. 2b and d, respectively).

In contrast to bone, which predominantly expresses type I collagen, fibrocartilage cells exhibit an intensely stained pericellular matrix that is enriched for type II collagen [13]. To further confirm the identity of the expanded cell population of enthesis fibrocartilage, we examined the immunohistochemical expression of type II collagen in enthesis fibrocartilage. As shown in Fig. 3a and consistent with previous findings, both the enthesis and calcaneal fibrocartilages of control mice are positive for type II collagen [14]. The identity of an expanded cell population into both the posterior and medial calcaneal tuberosity and the plantar fascia ligament attachment in Hyp mice as fibrocartilage was also confirmed by coll2-immunohistochemical staining (Fig. 3b).

The Expansion of Enthesis Fibrocartilage Is Due to an Increase in Mineralizing Fibrocartilage Cells

One of the key features of XLH-related enthesopathy is the mineralization of insertion sites. We therefore measured cellular AP activity as an indicator of cells actively involved in the mineralization of the fibrocartilage matrix [15]. In control mice, consistent with reports that the zone of mineralized fibrocartilage in the enthesis is quite small relative to total area, AP activity was confined to a small layer of cells in the Achilles insertion (Fig. 3c,Table 2) [9]. However, cells positive for AP activity of the Achilles insertion were elevated 10-fold in Hyp mice compared to control mice (Fig. 3d, Table 2) and corresponded to the localization of coll2-positive fibrocartilage cells shown in Fig. 3b. In addition, mineralized fibrocartilage cells were intensely positive for type X collagen, with pericellular matrix staining being relatively restricted to the immediate pericellular region (Fig. 3d, inset). Similarly, compared to AP activity of control quadriceps and patellar insertions (Fig. 4a, b), AP activity of the quadriceps and patellar insertions of Hyp mice were significantly higher (Fig. 4c and d, respectively; Table 2). Additionally, the von Kossa method for staining calcium mineral revealed that mineralization invades both the Achilles insertion and the plantar fascia ligament (Fig. 3e, f). Indeed, the highly irregular border of the mineralization front of both the Achilles and plantar fascia ligament were reminiscent of the mineralization front observed in the entheses of XLH patients, shown in Fig. 1. Finally, fibrocartilage cells aligned in rows, consistent with the thickened fibrocartilage shown in Fig. 3b and d, were especially evident in Hyp mice and discrete from bone mineral (Fig. 3g).

The Expansion of Fibrocartilage Is Evident During the Period of Fibrocartilage Development

The primary focus of our studies has been on older Hyp mice based on our observation that the enthesopathy of patients with XLH was progressive, occurring earliest in young adults. However, to better understand the progression and pathogenesis of the enthesopathy, we also examined the entheses of Hyp mice during the period of fibrocartilage development. We compared the entheses of 10-week-old mice, the period during which fibrocartilage develops and matures within the enthesis organ. We found, as has been described in the rat, that the Achilles insertion develops postnatally in mice [16,17]. At birth, the Achilles tendon is attached to the calcaneus, which is a cartilaginous model surrounded by a perichondrium (Fig. 5a). Evidence of fibrocartilage cells arranged in rows along with a metachromatic matrix becomes apparent by 2 weeks (Fig. 5b). The intensity of matrix staining continues to increase and becomes more restricted at 4 weeks, during which the secondary ossification center becomes evident within the calcaneus (Fig. 5c). AP activity was observed within type II collagen-positive fibrocartilage cells within the developing enthesis (Fig. 5d, e). Between 8 and 12 weeks, the secondary ossification centers mineralize into subchondral bone and the extracellular matrix between the rows of fibrocartilage cells becomes strongly meta-chromatic (Fig. 5f, g). We therefore examined and compared multiple fibrocartilaginous insertions of 10-week-old Hyp mice to those of control mice. Shown are the tibial insertion of the anterior cruciate ligament (Fig. 6a, b), the interosseous talocalcaneal ligament (Fig. 6c, d), the Achilles tendon (Fig. 6e, f), and the patellar tendon (Fig. 6g, h). In all sites examined, we observed an expansion of mineralized fibrocartilage cells during the period of fibrocartilage development, as evidenced by AP activity.

Enthesis Fibrocartilage Expresses the FGFR3 Receptor Subtype

The enthesopathy of XLH appears to be resistant to treatment of the underlying osteomalacia, suggesting that it is an inherent part of the disease. One key biochemical feature of XLH is the elevated circulating levels of the fibroblast growth factor FGF-23. FGF-23 is a phosphatonin that is elevated in XLH patients and Hyp mice and contributes to diminished bone mineralization by increasing urinary phosphate excretion and suppressing $1,25(OH)_2D_3$

production. Indeed, in contrast to wild-type mice (78 ± 23 pg/mL), serum levels of FGF-23 in Hyp mice were significantly higher at 898 ± 105 pg/mL. We tested the possibility that the high circulating levels of FGF-23 characteristic of XLH and Hyp mice may be part of the biochemical milieu that underlies the significant expansion of mineralizing enthesis fibrocartilage. FGF-23 is a putative ligand for the FGFR1 and FGFR3 receptor subtypes in renal epithelial cells [18,19]. We found that enthesis fibrocartilage does not express the FGFR1 receptor protein (Fig. 7a). However, the FGFR3 receptor protein was highly expressed in enthesis fibrocartilage (Fig. 7b) (as well as in proliferative growth plate chondrocytes, data not shown) and present in all fibrocartilaginous sites examined, including the Achilles and patellar fibrocartilage entheses. Klotho, a protein that forms a complex with several FGFR isoforms including FGFR3 and significantly increases their affinity for FGF-23, is also expressed in fibrocartilage cells (Fig. 7c) [20]. FGFR3 protein expression also persists in older control mice (Fig. 7d) and does not appear to be subject to downregulation in Hyp mice despite high circulating levels of FGF-23 (Fig. 7e). In addition, the elongated fibroblastic cells of the tendon (tenocytes) also stained positively for FGFR3 protein (Fig. 7f). These data provide a platform for the consideration that hormones such as FGF-23 may play a role in the changes we have described in the entheses of Hyp mice.

Discussion

We have demonstrated that enthesopathy characteristic of XLH occurs in the Hyp mouse, the best-known animal model of XLH. The primary histological feature of the enthesopathy of the Achilles and patellar insertion sites in this model is a dramatic cellular expansion and thickening of enthesis fibrocartilage. The Achilles insertion contains several functionally distinct fibrocartilaginous components, as is characteristic of many tendon insertion sites. Thus, the Achilles insertion site has been referred to as the prototypical “enthesis organ” by Benjamin and colleagues to describe the complex nature of these sites [8,14]. In addition to the enthesis fibrocartilage, the Achilles insertion contains a coll2-positive calcaneal fibrocartilage that, in concert with lubricating synovial fluid, reduces friction between the tendon and bone. The tendon is protected by a coll2-negative sesamoid fibrocartilage on the deep surface of the Achilles tendon, where the tendon presses against the superior tuberosity of the calcaneus in the dorsiflexed foot [21]. The enthesis fibrocartilage itself contains two zones: uncalcified and calcified. As has been previously described, we found that the zone of calcified fibrocartilage in the Achilles enthesis is quite narrow, as evidenced by the relatively small percentage of cells exhibiting AP activity in control mice. The increase in the percentage of AP-positive cells in Hyp mice is consistent with a recent study by Benjamin and coworkers [22] describing age-dependent enthesophyte formation in cadaver specimens and is consistent with previous observations of enthesopathies. The authors reported a significant thickening in the zone of mineralized fibrocartilage and the inclusion of bone nodules within the fibrocartilage. The bone nodules within the fibrocartilage did not appear to arise by typical endochondral bone formation as there was no cellular hypertrophy or significant vascular invasion present. Accordingly, we observed no evidence of vascularization using either specific antibodies against vascular markers or vascular endothelial growth factor (data not shown). It is possible that bone nodules might occur within the fibrocartilage of Hyp mice if allowed to progress further since the mean age of the patient study by Benjamin and coworkers [22] was 80 years. Fibrocartilage cells were, however, intensely positive for type X, with pericellular matrix staining being relatively restricted to the immediate pericellular region. Collagens play a number of regulatory roles in chondrocyte mineralization. Fibrillar collagens, like types I and II collagen, are cofactors for the propagation phase of hydroxyapatite formation, serving as a scaffold for crystal growth [23]. Type X collagen is a nonfibrillar collagen that is transiently synthesized and secreted by hypertrophic chondrocytes of the growth plate and may play a regulatory role in chondrocyte mineralization. In the growth plate, the progression of chondrocytes from proliferative to terminally differentiating stages is marked by a transition of predominantly type II collagen-

expressing cells to type X collagen-expressing cells [24]. Chondrocytes can directly interact with type X collagen via the $\alpha_1\beta_2$ integrin receptor, and assembly of type X collagen into a hexagonal network may accommodate the formation and/or restrict mineralization to terminally differentiated chondrocytes within the growth plate [25–27]. More recently, it has been shown that type II and type X collagen bind annexin V, which mediates calcium influx into matrix vesicles. Further, disruption of this interaction resulted in diminished AP activity and mineralization [28]. However, unlike growth plate chondrocytes, type X collagen (and AP) persists in fibrocartilage throughout adulthood, a finding we have confirmed [16,29,30]. The persistence of both proteins in enthesis fibrocartilage may reflect the unique role of mineralized fibrocartilage to impart mechanical strength to the load transfer that occurs at the muscle–bone interface. Finally, although not the focus of this study, examination of the entire thickness of the calcaneal fibrocartilage surface in serial sections from Hyp mice revealed a narrowing of the calcaneal fibrocartilage that normally comes into contact with the tendon and Kager's fat pad.

The enthesophytes observed in XLH patients occur decades earlier than those typically observed in the general population upon aging, a finding that we have confirmed. Indeed, this complication of XLH may represent one of the most significant correlates of progressive pain and debilitation occurring in middle-aged adults with the disease. In addition to the "aging process" in the normal adult population, the development of enthesopathy has been attributed to cumulative effects of mechanical loading. In addition, "overuse" enthesopathies in the general population are believed to develop in response to excessive or abnormal biomechanical forces [31]. It is, however, unclear whether the observed changes in the entheses of XLH patients and Hyp mice are due to changes in the mechanical and/or the biochemical environment as both have been described [2,32,33]. Enthesis fibrocartilage is especially adapted to accommodate the distribution of forces between the muscle–bone and bone–bone interfaces and are characterized by considerable tensile strength. Thus, the enthesis serves to minimize concentrated stress through this specialized functional role of fibrocartilage, thereby enabling load transfer between two distinct types of tissue (muscle and bone). Several anatomical features underlie the ability of fibrocartilage to function in this capacity. The unmineralized fibrocartilaginous matrix is rich in type II collagen, a fibrillar collagen that enables the enthesis to bend, while mineralized fibrocartilage consists primarily of types II and X collagen and aggrecan, which impart compressive strength [29]. While the zone between unmineralized and mineralized fibrocartilage is normally regular, the contrasting highly irregular pattern of mineralized fibrocartilage into the underlying bone matrix minimizes the stress between the fibrocartilage–bone interface. Because the tidemark is normally a region of mechanical weakness in both the enthesis and articular cartilage, it is possible that the transition of a normally smooth tidemark to a highly irregular one seen in both X-rays obtained from XLH patients and Hyp mice may be an adaptation to excessive forces [34].

That fibrocartilage is sensitive to mechanical force is almost intuitive, bolstered by observations that changes in load can alter the matrix profile of fibrocartilage [35,36]. In addition, studies by Thomopoulos et al. [37] demonstrate that postnatal development of supraspinatus enthesis fibrocartilage is impaired by decreased muscle loading, resulting in a significant decrease in enthesis fibrocartilage cells. It is also interesting to note, in light of the increase in fibrocartilage, that Benjamin and Ralphs [29] proposed that mechanical forces stimulate the metaplasia of tendon fibroblasts to fibrocartilage based on their observation of a positive correlation between the total area of fibrocartilage and the extent of movement of a particular insertion. Further, and as mentioned previously, the zone of calcified fibrocartilage is typically quite small and in intimate contact with the underlying bone. This raises the distinct consideration that the increase in fibrocartilage may actually contribute to altered mechanical forces. Even if the underlying osteomalacia were effectively treated, the significant increase

in these cells would be predicted to diminish the transfer of forces between what would be normally a thin zone of fibrocartilage and bone.

Changes in the biochemical environment may also contribute to the formation of enthesophytes. The early expansion of fibrocartilage cells, as observed in fibrocartilaginous insertion sites of 10-week-old animals, also suggests that the hyperplasia of cells may be driven by changes in the cellular milieu. Several phosphatonins circulate in patients with XLH and in Hyp mice in greater concentrations than in normal humans and mice. These substances include FGF-23 and matrix extracellular matrix glycoprotein (MEPE), which is highly upregulated in osteoblasts of Hyp mice [38]. MEPE belongs to the SIBLING family of proteins that contains an ASARM (serine- and aspartic acid–rich motif) motif, which is cleaved as the result of endopeptidase activity. The released ASARM product of MEPE has properties of both a phosphatonin in that it inhibits renal phosphate reabsorption and a direct inhibitor of hydroxyapatite formation [39,40]. In addition, because PHEX can proteolytically cleave ASARM peptides, it is thought that the PHEX mutation of Hyp mice contributes to hypomineralization of bone due to the accumulation of ASARM peptides [41]. It therefore seems unlikely that MEPE would play a role in the expansion of mineralized fibrocartilage in the Hyp model, given its mineralization-inhibitory properties. However, mineralization is a tightly regulated process that ensures an appropriate degree of mineralization as well as restriction to the appropriate tissue. Perhaps fibrocartilage cells are resistant to the direct effect of MEPE-derived ASARMs or, unlike the matrix vesicles derived from osteoblasts, matrix vesicles of cartilage cells do not secrete MEPE proteins. Thus, it is possible that such an inhibitory protein could underlie the inappropriate mineralization of the enthesis in a rachitic environment, but this seems unlikely given its described properties.

Results that fibrocartilage cells are highly positive for FGFR3/Klotho were entirely unexpected because gain-of-function mutations in FGFR3 are the most common cause of short-limbed dwarfism as a consequence of a decrease in the proliferative zone of chondrocytes [42,43]. This is supported by the finding that long bone overgrowth in FGFR3 knockout mice is due to an expansion of the proliferative zone and hypertrophic chondrocytes within the growth plate [44]. In that fibrocartilage cells share phenotypic markers of both fibroblasts and chondrocytes, we anticipated that expression of FGFR3 would not be associated with significant expansion of fibrocartilage. However, discrepancies between FGFR3 as an inhibitor of chondrocyte proliferation and the possibility of acting as a stimulator of fibrocartilage proliferation may arise from differences in the native ligand for the receptor. FGF-18 is the likely native ligand for growth plate chondrocytes, while we propose that the native ligand for fibrocartilage in XLH is FGF-23 [45]. Indeed, a relatively large number of FGF ligands signal via four distinct FGF receptor tyrosine kinesis, resulting in a diverse number of cellular responses [46]. There is also evidence that FGFR3 can function to both stimulate and inhibit proliferation depending upon the stage of chondrocyte development [47]. Alternatively, fibroblast growth factors stimulate the differentiation of a number of tissues and may do so in fibrocartilage [48]. It has been postulated that fibrocartilage cells arise by metaplasia (transdifferentiation) of tendon or ligament fibroblasts, which thus raises the possibility that the expansion of fibrocartilage is mediated by an increase in this transition [30,49]. We did, in fact, find that the fibroblast-like tenocytes were also positive for FGFR3 well into the proximal tendon. In addition, we found that the highest intensity of both FGFR3 and Klotho immunostaining was observed during the period of fibrocartilage cell differentiation in tissue samples ranging from newborn to 12 weeks.

As previously mentioned, several phosphate-wasting bone disorders are similarly characterized by high circulating levels of FGF-23. It will be of particular interest to determine if similar enthesis anomalies exist in other mouse models of osteomalacia with elevated levels of FGF-23, such as dentin matrix protein 1 (DMP1) knockout mice, a model of autosomal recessive hypophosphatemia rickets. In addition, because Dmp1-null mice have normal Phex expression,

they would also provide insight into a putative role that Phex may play in enthesopathy. The putative role of FGF-23 is currently being further explored.

Acknowledgments

We thank Nancy Troiano for technical assistance. We also thank the subjects participating in our clinical research protocols for their generous donation of time and effort, allowing the clinical characterization of features of the disease described here. Funding was provided by the NIH/NIAMSD (P50-AR054086-02) and the NIH/NIDDK (R01DK62515-26).

References

1. White KE, Carn G, Lorenz-Depiereux B, Benet-Pages A, Strom TM, Econs MJ. Autosomal-dominant hypophosphatemic rickets (ADHR) mutations stabilize FGF-23. Kidney Int 2001;60:2079–2086. [PubMed: 11737582]
2. Fukumoto S, Yamashita T. Fibroblast growth factor-23 is the phosphaturic factor in tumor-induced osteomalacia and may be phosphatonin. Curr Opin Nephrol Hypertens 2002;11:385–389. [PubMed: 12105387]
3. Bowe AE, Finnegan R, Jan de Beur SM, Cho J, Levine MA, Kumar R, Schiavi SC. FGF-23 inhibits renal tubular phosphate transport and is a PHEX substrate. Biochem Biophys Res Commun 2001;284:977–981. [PubMed: 11409890]
4. Feng JQ, Ward LM, Liu S, Lu Y, Xie Y, Yuan B, Yu X, Rauch F, Davis SI, Zhang S, Rios H, Drezner MK, Quarles LD, Bonewald LF, White KE. Loss of DMP1 causes rickets and osteomalacia and identifies a role for osteocytes in mineral metabolism. Nat Genet 2006;38:1310–1315. [PubMed: 17033621]
5. Lorenz-Depiereux B, Bastepe M, Benet-Pages A, Amyere M, Wagenstaller J, Muller-Barth U, Badenhoop K, Kaiser SM, Rittmaster RS, Shlossberg AH, Olivares JL, Loris C, Ramos FJ, Glorieux F, Vikkula M, Juppner H, Strom TM. DMP1 mutations in autosomal recessive hypophosphatemia implicate a bone matrix protein in the regulation of phosphate homeostasis. Nat Genet 2006;38:1248–1250. [PubMed: 17033625]
6. Polisson RP, Martinez S, Khoury M, Harrell RM, Lyles KW, Friedman N, Harrelson JM, Reisner E, Drezner MK. Calcification of entheses associated with X-linked hypophosphatemic osteomalacia. N Engl J Med 1985;313:1–6. [PubMed: 4000222]
7. Reid IR, Hardy DC, Murphy WA, Teitelbaum SL, Bergfeld MA, Whyte MP. X-linked hypophosphatemia: a clinical, biochemical, and histopathologic assessment of morbidity in adults. Medicine (Baltimore) 1989;68:336–352. [PubMed: 2811660]
8. Benjamin M, Kumai T, Milz S, Boszczyk BM, Boszczyk AA, Ralphs JR. The skeletal attachment of tendons–tendon “entheses”. Comp Biochem Physiol A Mol Integr Physiol 2002;133:931–945. [PubMed: 12485684]
9. Benjamin M, Toumi H, Ralphs JR, Bydder G, Best TM, Milz S. Where tendons and ligaments meet bone: attachment sites (“enthuses”) in relation to exercise and/or mechanical load. J Anat 2006;208:471–490. [PubMed: 16637873]
10. Ramonda R, Sfriso P, Podswiadek M, Oliviero F, Valvason C, Punzi L. The enthesopathy of vitamin D-resistant osteomalacia in adults [in Italian]. Reumatismo 2005;57:52–56. [PubMed: 15776147]
11. Benjamin M, Tyers RN, Ralphs JR. Age-related changes in tendon fibrocartilage. J Anat 1991;179:127–136. [PubMed: 1817130]
12. Yost JH, Spencer-Green G, Brown LA. Radiologic vignette, X-linked hypophosphatemia (familial vitamin D-resistant rickets). Arthritis Rheum 1994;37:435–438. [PubMed: 8129801]
13. Benjamin M, Evans EJ. Fibrocartilage. J Anat 1990;171:1–15. [PubMed: 2081696]
14. Benjamin M, Moriggl B, Brenner E, Emery P, McGonagle D, Redman S. The “enthesis organ” concept: why enthesopathies may not present as focal insertional disorders. Arthritis Rheum 2004;50:3306–3313. [PubMed: 15476254]
15. de Bernard B, Bianco P, Bonucci E, Costantini M, Lunazzi GC, Martinuzzi P, Modricky C, Moro L, Panfili E, Pollesello P, et al. Biochemical and immunohistochemical evidence that in cartilage an

alkaline phosphatase is a Ca^{2+}-binding glycoprotein. J Cell Biol 1986;103:1615–1623. [PubMed: 3771650]

16. Fujioka H, Wang GJ, Mizuno K, Balian G, Hurwitz SR. Changes in the expression of type-X collagen in the fibrocartilage of rat Achilles tendon attachment during development. J Orthop Res 1997;15:675–681. [PubMed: 9420596]
17. Rufai A, Ralphs JR, Benjamin M. Structure and histopathology of the insertional region of the human Achilles tendon. J Orthop Res 1995;13:585–593. [PubMed: 7674075]
18. Liu S, Vierthaler L, Tang W, Zhou J, Quarles LD. FGFR3 and FGFR4 do not mediate renal effects of FGF-23. J Am Soc Nephrol 2008;19:2342–2350. [PubMed: 18753255]
19. Urakawa I, Yamazaki Y, Shimada T, Iijima K, Hasegawa H, Okawa K, Fujita T, Fukumoto S, Yamashita T. Klotho converts canonical FGF receptor into a specific receptor for FGF-23. Nature 2006;444:770–774. [PubMed: 17086194]
20. Kurosu H, Ogawa Y, Miyoshi M, Yamamoto M, Nandi A, Rosenblatt KP, Baum MG, Schiavi S, Hu MC, Moe OW, Kuro-o M. Regulation of fibroblast growth factor-23 signaling by klotho. J Biol Chem 2006;281:6120–6123. [PubMed: 16436388]
21. Rufai A, Benjamin M, Ralphs JR. Development and ageing of phenotypically distinct fibrocartilages associated with the rat Achilles tendon. Anat Embryol (Berl) 1992;186:611–618. [PubMed: 1292376]
22. Benjamin M, Toumi H, Suzuki D, Hayashi K, McGonagle D. Evidence for a distinctive pattern of bone formation in enthesophytes. Ann Rheum Dis 2009;68:1003–1010. [PubMed: 18625624]
23. Murshed M, Harmey D, Millan JL, McKee MD, Karsenty G. Unique coexpression in osteoblasts of broadly expressed genes accounts for the spatial restriction of ECM mineralization to bone. Genes Dev 2005;19:1093–1104. [PubMed: 15833911]
24. Broadus AE, Macica C, Chen X. The PTHrP functional domain is at the gates of endochondral bones. Ann N Y Acad Sci 2007;1116:65–81. [PubMed: 18083922]
25. Jacenko O, Chan D, Franklin A, Ito S, Underhill CB, Bateman JF, Campbell MR. A dominant interference collagen X mutation disrupts hypertrophic chondrocyte pericellular matrix and glycosaminoglycan and proteoglycan distribution in transgenic mice. Am J Pathol 2001;159:2257–2269. [PubMed: 11733375]
26. Kwan AP, Cummings CE, Chapman JA, Grant ME. Macromolecular organization of chicken type X collagen in vitro. J Cell Biol 1991;114:597–604. [PubMed: 1860888]
27. Luckman SP, Rees E, Kwan AP. Partial characterization of cell-type X collagen interactions. Biochem J 2003;372:485–493. [PubMed: 12617725]
28. Kim HJ, Kirsch T. Collagen/annexin V interactions regulate chondrocyte mineralization. J Biol Chem 2008;283:10310–10317. [PubMed: 18281278]
29. Benjamin M, Ralphs JR. Fibrocartilage in tendons and ligaments—an adaptation to compressive load. J Anat 1998;193:481–494. [PubMed: 10029181]
30. Benjamin M, Ralphs JR. Entheses—the bony attachments of tendons and ligaments. Ital J Anat Embryol 2001;106:151–157. [PubMed: 11729950]
31. Benjamin M, Rufai A, Ralphs JR. The mechanism of formation of bony spurs (enthesophytes) in the Achilles tendon. Arthritis Rheum 2000;43:576–583. [PubMed: 10728751]
32. Camacho NP, Rimnac CM, Meyer RA Jr, Doty S, Boskey AL. Effect of abnormal mineralization on the mechanical behavior of X-linked hypophosphatemic mice femora. Bone 1995;17:271–278. [PubMed: 8541141]
33. Meyer RA Jr, Meyer MH, Gray RW, Bruns ME. Femoral abnormalities and vitamin D metabolism in X-linked hypophosphatemic (Hyp and Gy) mice. J Orthop Res 1995;13:30–40. [PubMed: 7853101]
34. Shaw HM, Benjamin M. Structure–function relationships of entheses in relation to mechanical load and exercise. Scand J Med Sci Sports 2007;17:303–315. [PubMed: 17490450]
35. Evanko SP, Vogel KG. Proteoglycan synthesis in fetal tendon is differentially regulated by cyclic compression in vitro. Arch Biochem Biophys 1993;307:153–164. [PubMed: 7694546]
36. Koob TJ, Clark PE, Hernandez DJ, Thurmond FA, Vogel KG. Compression loading in vitro regulates proteoglycan synthesis by tendon fibrocartilage. Arch Biochem Biophys 1992;298:303–312. [PubMed: 1524441]

37. Thomopoulos S, Kim HM, Rothermich SY, Biederstadt C, Das R, Galatz LM. Decreased muscle loading delays maturation of the tendon enthesis during postnatal development. J Orthop Res 2007;25:1154–1163. [PubMed: 17506506]
38. Argiro L, Desbarats M, Glorieux FH, Ecarot B. Mepe, the gene encoding a tumor-secreted protein in oncogenic hypophosphatemic osteomalacia, is expressed in bone. Genomics 2001;74:342–351. [PubMed: 11414762]
39. Rowe PS, Kumagai Y, Gutierrez G, Garrett IR, Blacher R, Rosen D, Cundy J, Navvab S, Chen D, Drezner MK, Quarles LD, Mundy GR. MEPE has the properties of an osteoblastic phosphatonin and minhibin. Bone 2004;34:303–319. [PubMed: 14962809]
40. Addison WN, Nakano Y, Loisel T, Crine P, McKee MD. MEPE-ASARM peptides control extracellular matrix mineralization by binding to hydroxyapatite: an inhibition regulated by PHEX cleavage of ASARM. J Bone Miner Res 2008;23:1638–1649. [PubMed: 18597632]
41. Rowe PS, Garrett IR, Schwarz PM, Carnes DL, Lafer EM, Mundy GR, Gutierrez GE. Surface plasmon resonance (SPR) confirms that MEPE binds to PHEX via the MEPE-AS-ARM motif: a model for impaired mineralization in X-linked rickets (HYP). Bone 2005;36:33–46. [PubMed: 15664000]
42. Colvin JS, Bohne BA, Harding GW, McEwen DG, Ornitz DM. Skeletal overgrowth and deafness in mice lacking fibroblast growth factor receptor 3. Nat Genet 1996;12:390–397. [PubMed: 8630492]
43. Deng C, Wynshaw-Boris A, Zhou F, Kuo A, Leder P. Fibroblast growth factor receptor 3 is a negative regulator of bone growth. Cell 1996;84:911–921. [PubMed: 8601314]
44. Eswarakumar VP, Schlessinger J. Skeletal overgrowth is mediated by deficiency in a specific isoform of fibroblast growth factor receptor 3. Proc Natl Acad Sci USA 2007;104:3937–3942. [PubMed: 17360456]
45. Davidson D, Blanc A, Filion D, Wang H, Plut P, Pfeffer G, Buschmann MD, Henderson JE. Fibroblast growth factor (FGF) 18 signals through FGF receptor 3 to promote chondrogenesis. J Biol Chem 2005;280:20509–20515. [PubMed: 15781473]
46. Dailey L, Ambrosetti D, Mansukhani A, Basilico C. Mechanisms underlying differential responses to FGF signaling. Cytokine Growth Factor Rev 2005;16:233–247. [PubMed: 15863038]
47. Iwata T, Chen L, Li C, Ovchinnikov DA, Behringer RR, Francomano CA, Deng CX. A neonatal lethal mutation in FGFR3 uncouples proliferation and differentiation of growth plate chondrocytes in embryos. Hum Mol Genet 2000;9:1603–1613. [PubMed: 10861287]
48. Eswarakumar VP, Lax I, Schlessinger J. Cellular signaling by fibroblast growth factor receptors. Cytokine Growth Factor Rev 2005;16:139–149. [PubMed: 15863030]
49. Gao J, Messner K, Ralphs JR, Benjamin M. An immunohistochemical study of enthesis development in the medial collateral ligament of the rat knee joint. Anat Embryol (Berl) 1996;194:399–406. [PubMed: 8896704]

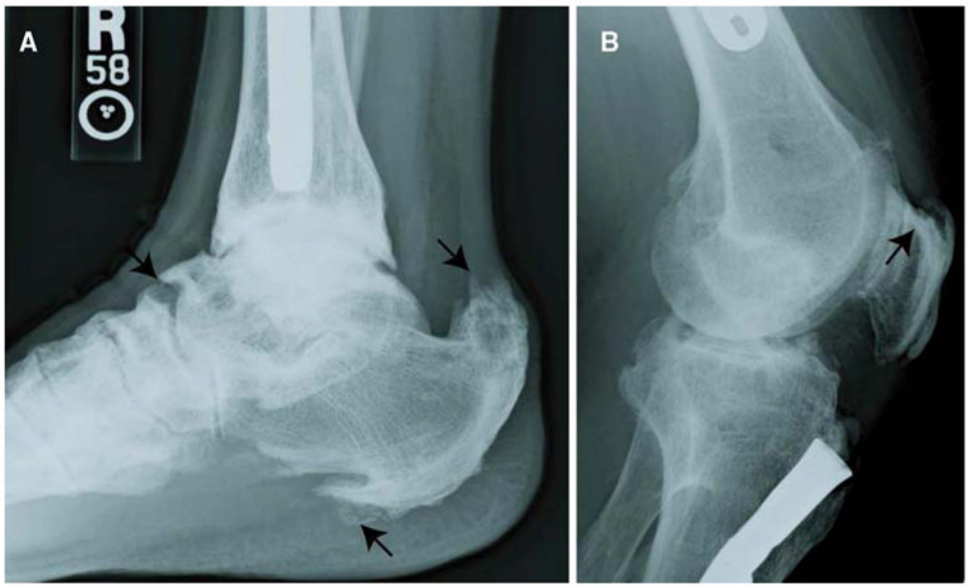

Fig. 1.

Enthesophyte formation in XLH patients. **a** Enthesophytes at the site of enthesis attachment to the plantar aspect of the calcaneus are evident. Prominent enthesopathy and progressive mineralization at the site of the Achilles tendon are marked by *arrows*. **b** Calcification of the patellar ligament insertion is shown by the *arrow*. Note the fusion of the patella to the femur

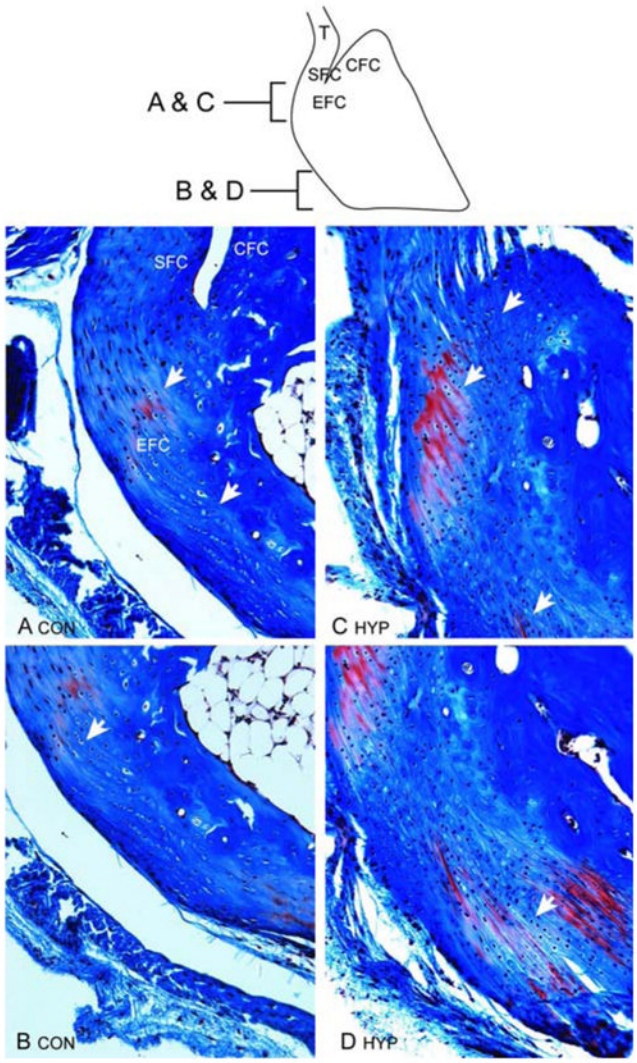

Fig. 2.

Achilles insertion into the tuberosity of the calcaneus of control and Hyp mice; sagittal sections stained with Masson's trichrome. **a, b** As shown schematically (SFC, sesamoid fibrocartilage; CFC, calcaneal fibrocartilage; EFC, enthesis fibrocartilage), fibrocartilage cells of the enthesis of age-matched control mice are mostly confined to the proximal calcaneus. **c, d** Expansion of fibrocartilage cells (identified by rows of cells aligned between collagen fibers) of Achilles insertion of Hyp mice extend across the posterior surface of the proximal insertion into the CFC (**c**) and well into the distal tuberosity (**d**)

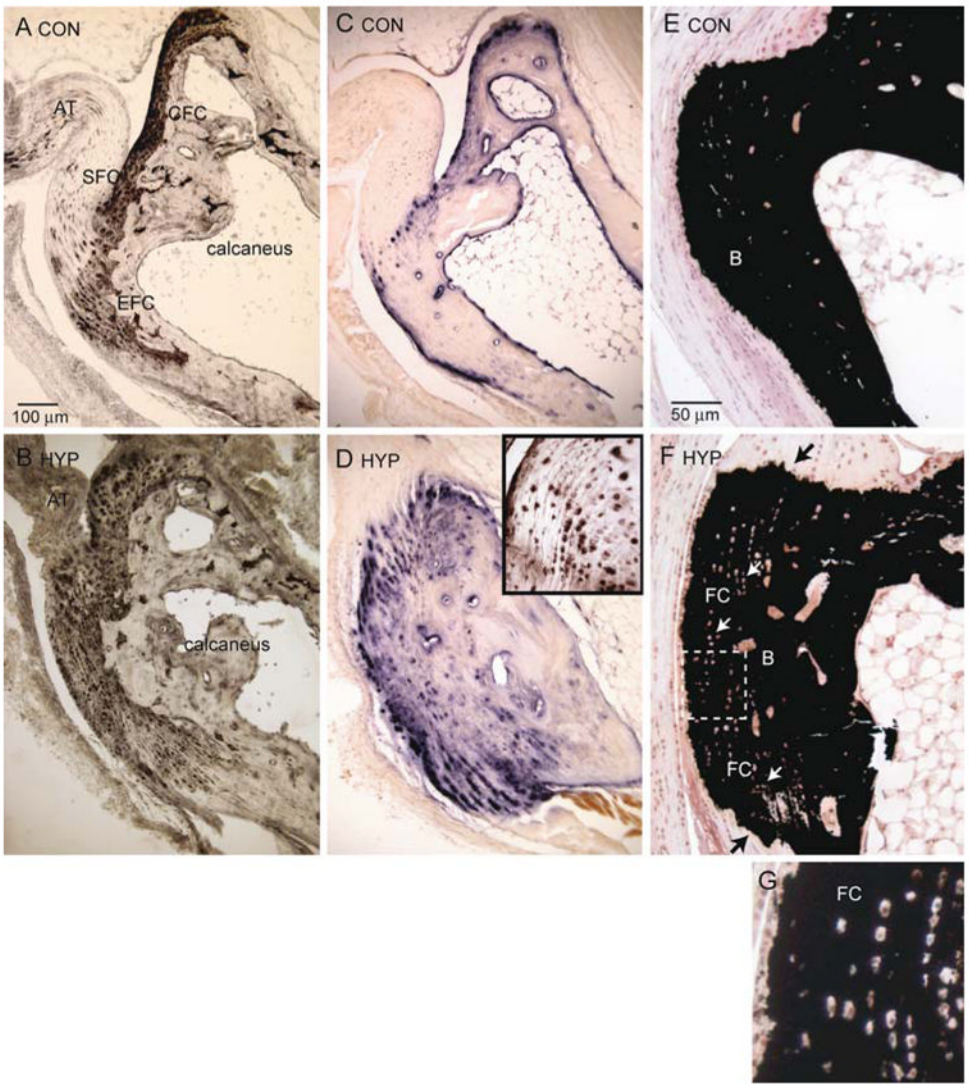

Fig. 3.

Cellular expansion of mineralizing fibrocartilage in Hyp mice. Achilles insertion into the tuberosity of the calcaneus of control and Hyp mice. **a** Control mice; immunohistochemical staining of type 2 collagen (coll2) of the Achilles enthesis organ is confined to the calcaneal fibrocartilage (CFC) and enthesis fibrocartilage (EFC). **b** Hyp mice; expansion of EFC into the posterior and medial process of the calcaneus. Fibrocartilage (FC) is also prominent at the plantar fascia ligament attachment. **c** Control mice; cellular AP of EFC is confined to the zone of mineralized fibrocartilage. **d** Hyp mice; expansion of cellular AP activity colocalizes with type 2 collagen-positive fibrocartilage cells shown in **b**. *Inset*: Fibrocartilage cells, a marker of hypertrophic chondrocytes, are also positive for type X collagen. **e** Control mice; von Kossa staining of calcium mineral predominantly corresponds with bone mineral shown in **c. f** Hyp mice; von Kossa staining of bone mineral (B) and fibrocartilage mineral (FC). *Black arrows* show that mineralization invades both the Achilles insertion and the plantar fascia ligament; *white arrows* show fibrocartilage cells. **g** Fibrocartilage cells (at higher magnification) aligned in rows were especially evident in Hyp mice and discrete from bone mineral (**c, f**) of control and Hyp mice

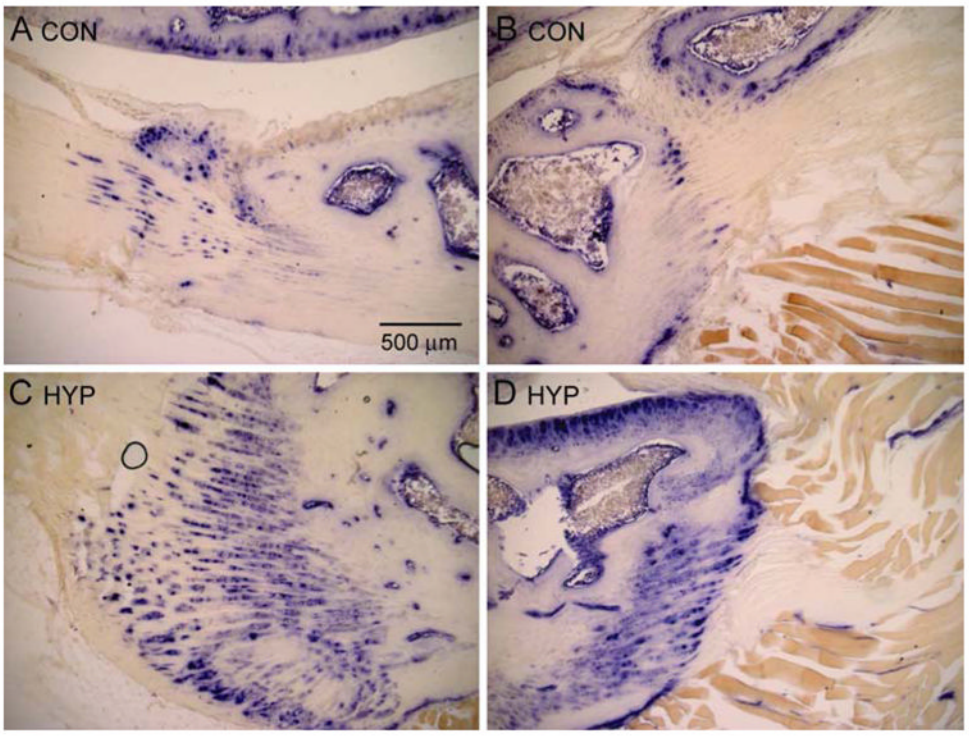

Fig. 4.

Cellular expansion of mineralizing fibrocartilages in patellar insertions. Cellular AP activity of the quadriceps femoris tendon insertion into the patella and patellar attachment of the patellar ligament of control and Hyp mice. **a** Control mice; AP activity of mineralized fibrocartilage of quadriceps insertion. **b** Control mice; AP activity of mineralized fibrocartilage of patellar insertion. **c** Hyp mice; AP activity of mineralized fibrocartilage of quadriceps insertion. **d** Hyp mice; AP activity of mineralized fibrocartilage of patellar insertion. Note considerable expansion of AP-positive fibrocartilage in Hyp mice

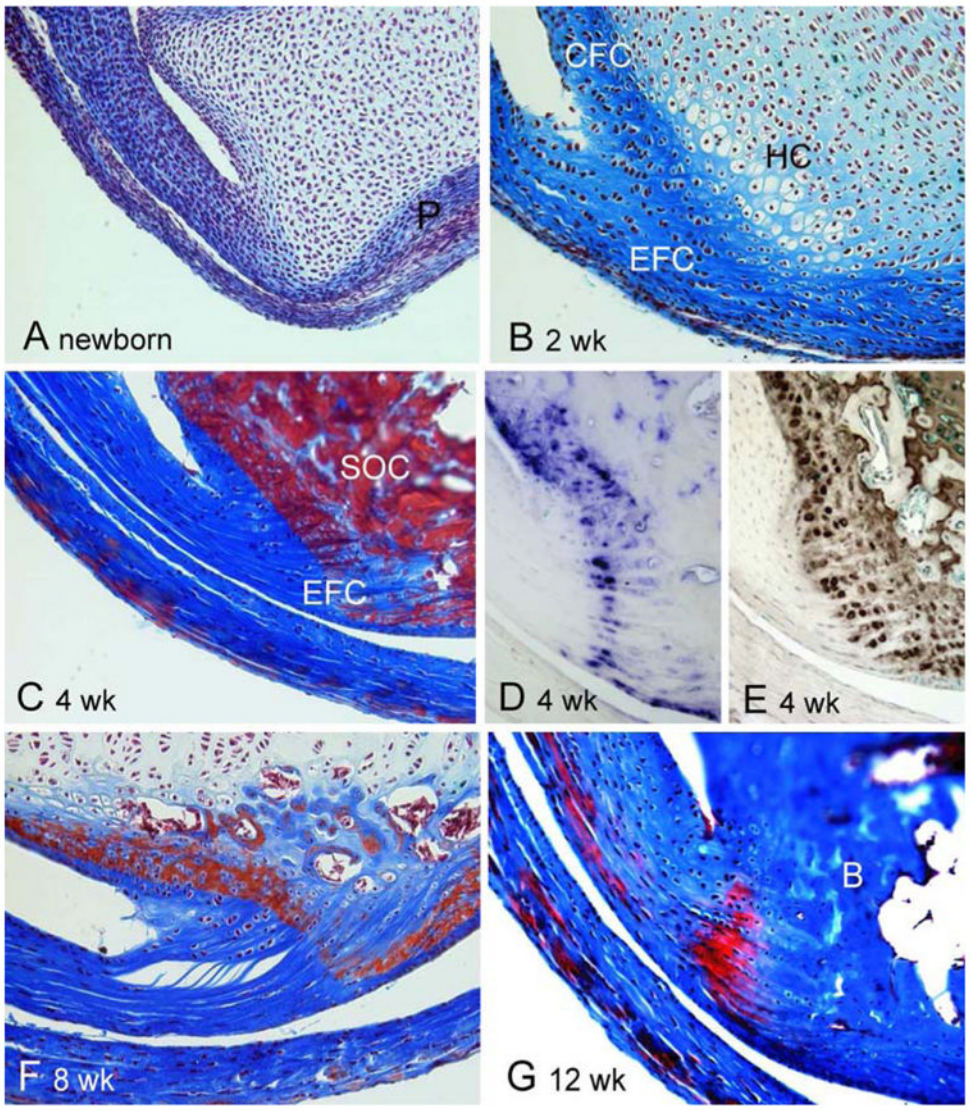

Fig. 5.

Development of Achilles tendon insertion in mice. **a** At birth, the Achilles tendon is attached to a cartilaginous model of the calcaneus, which is surrounded by a perichondrium (P). **b** At 2 weeks, fibrocartilage cells of the enthesis (EFC) are arranged in rows and characterized by a metachromatic pericellular matrix. Matrix-positive calcaneal fibrocartilage (CFC) also becomes evident. Cartilage cells within the calcaneus show evidence of hypertrophy (HC). **c** The intensity of matrix staining continues to increase and becomes more restricted at 4 weeks, during which the secondary ossification center (SOC) becomes evident within the calcaneus. **d** At 4 weeks, AP activity is associated with EFC and CFC. **e** At 4 weeks, type II collagen is expressed in both EFC and CFC. **f** At 8 weeks, the secondary ossification center begins to mineralize and is replaced by subchondral bone and the extracellular matrix between the rows of fibrocartilage cells becomes strongly metachromatic. **g** At 12 weeks, the subchondral bone matrix (B) is intensely stained and distinguishable from the somewhat less intensely stained mineralized fibrocartilage

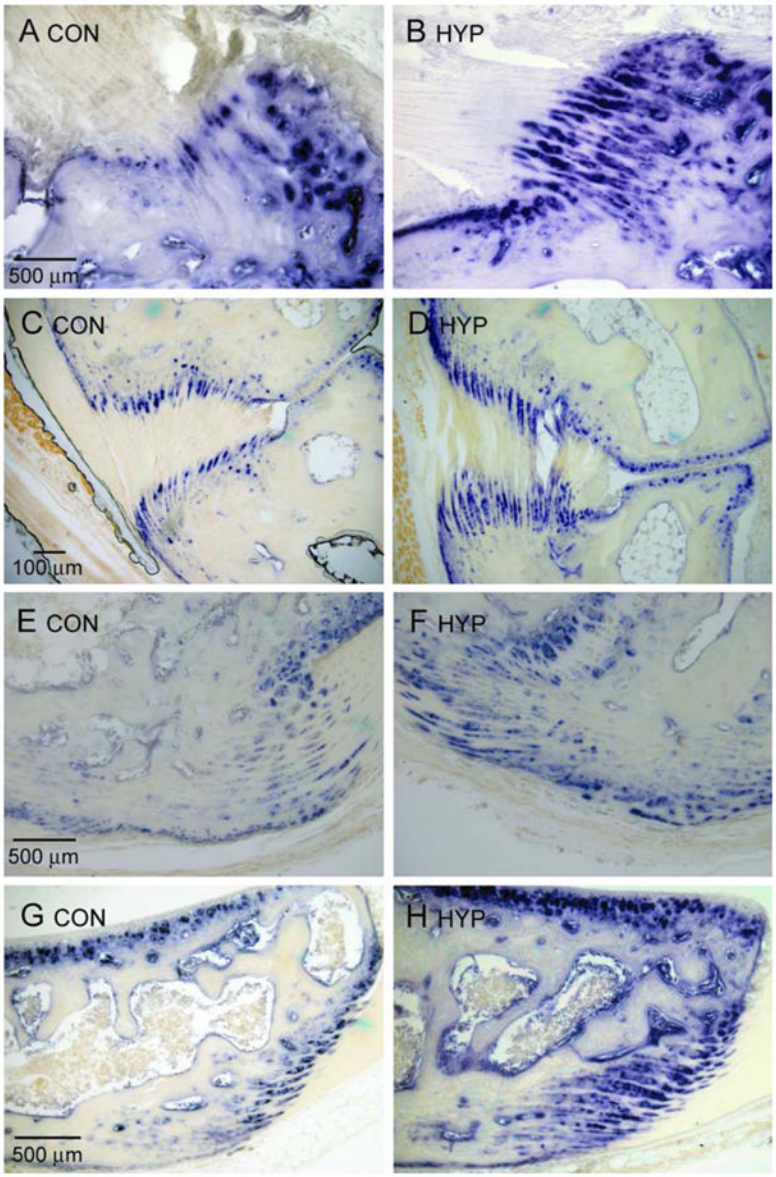

Fig. 6.

AP activity of fibrocartilaginous insertions of 10-week-old control (Con) and Hyp mice. (**a, b**) AP-positive mineralized fibrocartilage is expanded in the tibial insertion of the anterior cruciate ligament of Hyp mice, relative to control mice, as well as in the interosseous talocalcaneal ligament (**c, d**), the Achilles tendon (**e, f**), and the patellar tendon (**g, h**) of Hyp mice

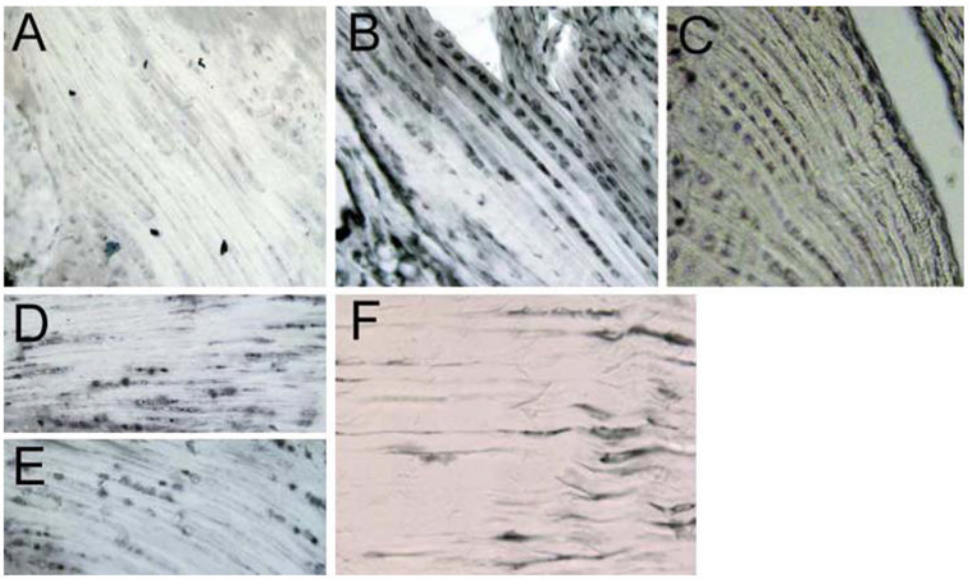

Fig. 7.

Enthesis fibrocartilage expresses FGFR3. **a** Immunohistochemical localization showing the absence of FGFR1 in fibrocartilage (12-week-old mouse). **b** Serial section of tissue shown in **a**, showing the presence of FGFR3 in fibrocartilage. **c** Immunohistochemical localization of the FGFR coreceptor Klotho to enthesis fibrocartilage. **d, e** Persistent expression of FGFR3 and Klotho in enthesis fibrocartilage from 7-month-old mice. **f** Tenocytes proximal to fibrocartilage also express FGFR3

Table 1

Extent of enthesopathy in humans with XLH: 39 patients were examined at all sites except the spine, for which 29 subjects were examined

Site	Shoulder	Elbow	Pelvis	Knee	Ankle	Hand	Spine
Affected patients, *n* (%)	3 (8)	11 (28)	19 (49)	22 (56)	29 (74)	11 (28)	12 (41)

Calcif Tissue Int. Author manuscript; available in PMC 2010 November 19.

Table 2

Percentage of mineralizing fibrocartilage cells positive for AP activity of selected entheses, expressed as mean ± SD, $P < 0.01$

Insertion	Achilles	Quadriceps	Patellar
Control	5.3 ± 0.6%, $n = 8$	6.8 ± 2.2%, $n = 8$	9.8 ± 1.9%, $n = 8$
Hyp	57 ± 8.0%, $n = 8$	30.4 ± 3.3%, $n = 8$	17.7 ± 1.6%, $n = 8$